Truss Analogy for Steel Moment Connections

SUBHASH C. GOEL, BOŽIDAR STOJADINOVIĆ and KYOUNG-HYEOG LEE

INTRODUCTION

Unprecedented widespread failure of welded moment connections in steel frames caused by the 1994 Northridge and the 1995 Kobe earthquakes have alarmed the engineering communities throughout the world. Beam-to-column connections in steel frames have been traditionally designed by using classical Euler-Bernoulli beam theory which leads to assumptions that the flanges transfer moment while the web connection primarily resists the shear force.

The results of a recent finite element study at The University of Michigan have shown that stress distribution in the vicinity of moment connections drastically differs from the pattern assumed following the classical beam theory. This is in agreement with the boundary effect postulate expressed by the famous Saint Venant's Principle. The finite element study has shown that the magnitude and direction of the principal stresses in the connection region are better approximated by using truss analogy rather than the classical beam theory. Accordingly, both the bending moment and the shear force are transferred across the connection near the beam flanges through diagonal strut action. Thus, the beam flange region of the traditionally designed connection is overloaded. This conclusion explains, to a large extent, the recently observed steel moment connection failures.

This study uses the finite element analysis results and the truss analogy in order to establish a more realistic load path in the welded steel moment connections, a practical and more rational analysis and design procedure has been developed. The new connection design uses a combination of flange cover plates and vertical rib plates to carry the normal and shear stresses created by the truss action. The design procedure was successfully validated through cyclic load testing of a nearly full size specimen. The results show that the connection withstood more than 40 displacement cycles up to a maximum story drift of over 4 percent and a plastic rotations greater than 0.04 radian. As per design, the plastic hinge formed in the beam away from the connection with no significant yielding in the connection region. The specimen sustained a very demanding deformation history without developing any cracks anywhere.

The results of the finite element study, the new connection design procedure and the observations of the behavior of the specimen are briefly presented in this paper. More details can be found in the original report by the writers.

Subhash C. Goel is professor, Department of Civil & Environmental Engineering, The University of Michigan, Ann Arbor, MI.

Božidar Stojadinović is assistant professor, Department of Civil & Environmental Engineering, The University of Michigan, Ann Arbor, MI.

Kyoung-Hyeog Lee is doctoral candidate, Department of Civil & Environmental Engineering, The University of Michigan, Ann Arbor, MI.

STRESS DISTRIBUTION

The study began by re-examination of the behavior and performance of some beam-to-column sub-assemblies that were tested within the SAC Joint Venture research program.[2,3] A specimen used in the first series of full-scale tests[4] conducted after the Northridge earthquake was selected for detailed study. Dimensions and member sizes of the specimen are shown in Figure 1. The connection failed at a load of approximately 200 kips in a brittle manner typical of the failures observed during the Northridge earthquake.[5-7]

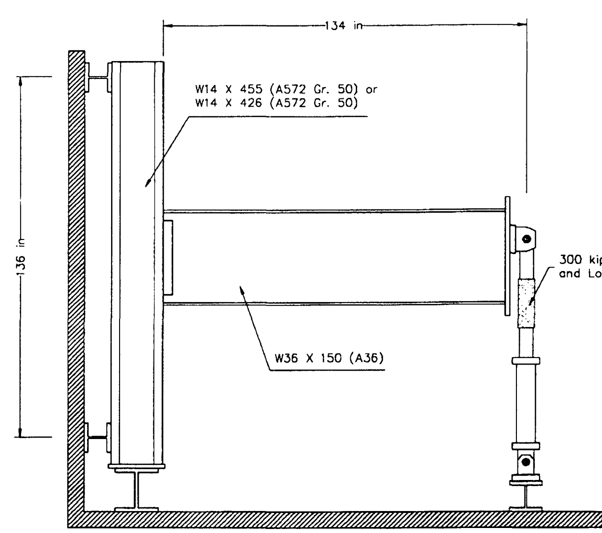

Fig. 1. Prototype beam-to-column connection assembly.

The stress distribution at a state near the failure load was studied on a finite element model of the specimen. The beam flanges and the web were assumed to be directly welded to the column flange to simplify the analysis. The distribution of Von Mises stress in the plane of the beam and column webs is shown in Figure 2. It is clear that the distribution of stresses some distance away from the column face agrees with that obtained using the classical Euler-Bernoulli hypothesis of plane sections. In contrast, the stress distribution changes drastically in the vicinity of the connection.

The distribution of stresses in the beam web is noteworthy. The classical parabolic distribution of shear stresses changes entirely near the connection. The area in the middle of the web near the shear tab is virtually devoid of stresses, while high stress concentrations occur in the flanges and the flange welds. Attention to this problem was drawn as early as 1934.[8] Later, the same problem was examined analytically, using finite element models, by Abel and Popov,[9] and experimentally by Popov and Pinkney[10] and Popov and Stephen.[11] On the column side of the connection stresses increase in the panel zone and in the column flanges near the welds.

Influence of the boundary conditions on the distribution of stresses and strains in the vicinity of the connection is obvious. The distribution of stresses is governed not only by the imposed loading (the traction boundary condition) but also by the deformation constraints imposed by the connection details (the displacement boundary condition). Theoretical foundation for this conclusion can be found in Timoshenko and Goodier, 1951.[12] The plane stress solution of a beam cantilever problem shows that shearing distorts, warps, the beam cross section. Traditional welded steel moment connection details prevent free deformation of the top and bottom fibers of the beam. Such boundary conditions constrain warping of the beam cross section and cause stretching that results in a redistribution of stresses and strains.

The well known Saint-Venant's Principle states:

> The replacement of forces acting on a small portion of the surface of an elastic body by another statically equivalent system of forces acting on the same portion of the surface produces substantial changes in the local stress distribution but has a negligible effect on the stresses at distances which are large in comparison with the linear dimensions of the surface on which the forces are acting.

This principle makes it possible to design the beam and the column away from the connection region by using the classical Euler-Bernoulli hypothesis. At the same time, the Saint-Venant's Principle also suggests that the connection region can not be designed by using the Euler-Bernoulli hypothesis.

A realistic stress or force distribution model, a load path model, is needed to design or analyze the connection region. The results of this and other[13,14] finite element studies show that the distribution of stresses in the connection is complex. In addition, the distribution of stresses and the intensity of stress concentrations can be quite sensitive to the choice of connection details. Therefore, a simplified load path or stress flow model must be formulated to derive a practical design procedure.

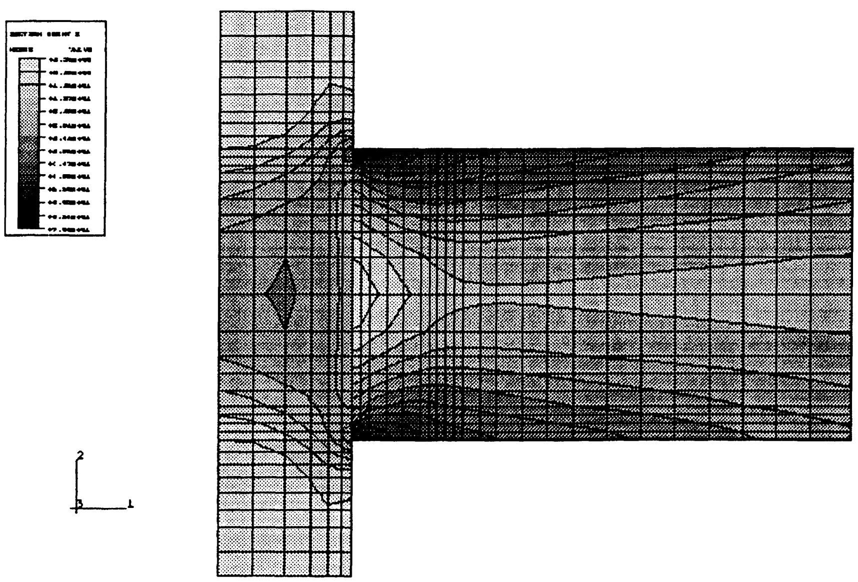

Fig. 2. Von Misses stress distribution.

TRUSS ANALOGY MODEL

The distribution of Von Mises stresses in the beam web of a typical pre-Northridge connection was shown in Figure 2. Directions and magnitudes of the corresponding principal stress vectors are shown in Figure 3. Both figures clearly indicate that the resultants of normal and shear stresses in the beam web form two diagonal struts that go through the corners of the beam near the flange welds. This observation inspired the use of truss analogy to model the load path through the moment connection. The truss analogy is an accepted tool for analysis and design of reinforced concrete structural elements.[15,16] Recently, truss models have also been proposed for analysis and design of bracing member connections in steel structures by Astaneh[17] and Bursi.[18,19]

The force path for the beam moment and shear forces in the vicinity of the connection is modeled by a statically admissible truss model, shown in Figure 4. In this truss model, the beam moment is transferred through the flanges acting as chords of the truss, while the shear force is carried by the truss diagonals. Clearly, the forces induced by the beam moment and shear are reacting against the top and bottom corners of the beam in the connection region. These corner areas need to be designed to resist both the horizontal and the vertical reaction forces. The middle of the beam web does not need to be connected to the column, since no load passes through that region of the connection.

The load path assumed using the truss analogy (Figure 4) is distinctly different from the load path postulated by the classical Euler-Bernoulli hypothesis. The classical load path assumes that the entire shear force along with some portion of the beam moment is transferred through the connection between the beam web and the column.

The truss model clearly shows that the force transferred through the flange welds is a vector sum of the horizontal force produced by the beam moment couple and the horizontal and vertical components of the diagonal shear strut force. Thus, the flange welds have to transfer both axial and shear stress and may be overloaded.[11] Furthermore, the column flange restrains the in-plane deformation of the weld, creating a tri-axial stress and strain state in the weld. Such stress-strain state is shown to severely reduce both the ductility and the strength of the weld material.[13,20] This combination of complex stress-strain state and overloading is, perhaps, the principal cause of premature brittle failures at or near the beam flange welds. The truss model also explains larger number of observed failures near the bottom flange of the beam: the presence of the deck on the top beam flange provides significant resistance to the vertical component of the diagonal strut force.

PROPOSED DESIGN PROCEDURE

The truss analogy model for the load path in moment connections makes it possible to formulate a simple, practical design procedure. According to this model, a designer simply needs to provide connections near the top and the bottom flange of the beam that can transfer the horizontal force due to the connection moment and the vertical force due to the connection shear. These flange connections should normally consist of a combination of horizontal and vertical plates, since the horizontal force can be conveniently carried through horizontal plates, while the vertical plates are much more efficient in

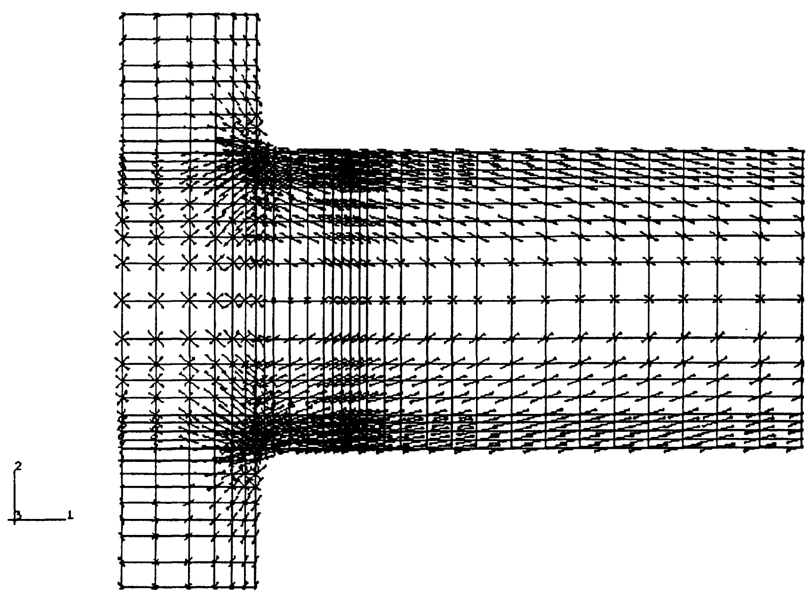

Fig. 3. Principal stress trajectories.

carrying the vertical force. The middle portion of the beam web need not be connected, except for a nominal connection used during erection. A possible connection arrangement is shown in Figure 5. The middle portion of the beam web need not be connected, except for a nominal connection used for erection purposes. The nominal connection may be designed to carry the full gravity led of the beam. Details of such connections were not considered in the study.

For adequate ductility in seismic resistant moment frames it is desirable that plastic hinges form in the beams at a safe distance from the beam-to-column connection region. Therefore, the beam-to-column connection needs to be designed to develop the maximum anticipated capacity of the beam at the location of the plastic hinge.[21]

The design process starts by selecting the beam section. Then, it is necessary to estimate the probable location and the capacity of the beam plastic hinges that could form in the event of a major earthquake. The horizontal and the vertical connection reaction forces at the column face can be obtained from a static analysis of the truss model constructed between the plastic hinge and the face of the column, as shown in Figure 4. Alternatively, in case of conventional force-based design, the connection design forces can also be calculated from the free body diagram of the beam by first computing the expected moment and shear forces at the face of the column. If the top and bottom flange connections are identical, the vertical connection reaction can be divided equally between the two. The moment part of the horizontal connection reaction force can be calculated by dividing the applied moment value by the distance between the centroids of the top and the bottom flange connections.

Each flange connection is designed for a horizontal, normal force and a vertical, shear force. The normal stress can be calculated by dividing the horizontal connection reaction force by the total area of all of the connection plates. The shear stress in the vertical plates can be conservatively calculated by dividing the vertical connection reaction force by the corresponding area of the vertical plates only. The horizontal plates of the flange connection and their welds may be designed for the normal stress only. The vertical plates and their welds need to be designed for combined normal and shear stresses by using appropriate design criteria. In both cases, the design criteria are based on the assumption of uniform stress distribution.

DESIGN OF THE TEST SPECIMEN

A pilot test specimen was designed to verify the proposed load path concept and the design procedure discussed above. The specimen was modeled after a full scale beam-to-column assembly specimen tested by Engelhardt.[4] The capacity of the loading frame required the specimen be scaled down by a one-third strength (force) ratio, meaning the length scaling ratio was approximately $1{:}\sqrt{3}$. However, every effort was made to preserve the geometric proportions of the prototype. The final design of the specimen is shown in Figure 6. The column, made of W12×152 A572 Gr. 50 118.5 inches long section, was bolted to the loading frame at each end, leaving a clear span of 84 inches between the supports. This column section was chosen to prevent shear yielding of the panel zone and make flexural yielding of the beam the primary source of inelastic deformation of the specimen. The beam was made of W21×50 dual grade (A36 and A572 Gr. 50) section. It represents half of one complete, scaled-down span. One end of the beam was moment-connected to the column. The other, free end of the beam was used to model the inflection point of the beam in a prototype frame with no gravity loads. The

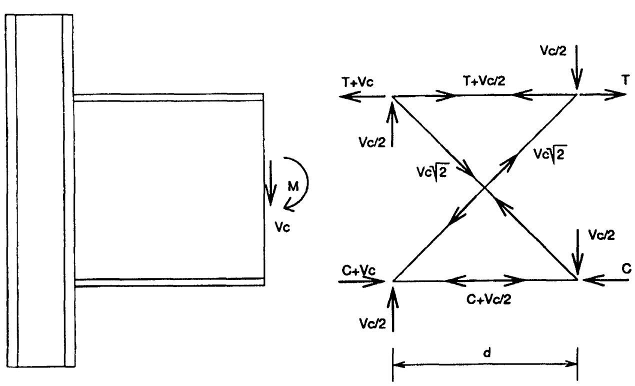

Fig. 4. Connection truss model.

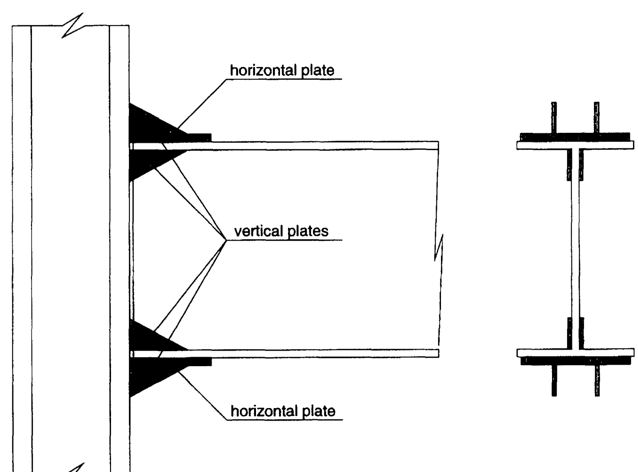

Fig. 5. A possible configuration of the new beam-to-column connection.

seismic shear load was applied at the free end of the beam using a pin. The distance between the pin and the column face was 84 inches.

The beam-to-column connection was designed by using the proposed procedure and the AISC LRFD Specification.[22] The flange connections were made by using horizontal flange cover plates and vertical triangular rib plates welded to the beam section and the column flange (Figures 7 and 8). The beam was not welded directly to the column at any point. This was done to minimize stress concentrations. The design calculations are briefly given in the following.

The location of the plastic hinge was assumed to be at a distance $d = 21$ inches (equal to the beam depth) from the face of the column (Figure 9). The probable plastic moment capacity of the beam, M_{pr}, was computed using Equation 6-1 of the SAC/FEMA Interim Guidelines:[2]

$$M_{pr} = 0.95 a F_{ya} Z_b = 6{,}793 \text{ kip-in} \quad (1)$$

where

a = coefficient that accounts for the effects of strain hardening and modeling uncertainty, taken as 1.3

F_{ya} = expected yield strength of the beam web material, taken as 50 ksi

Z_b = plastic section modulus of the beam section, equal to 110 in^3.

The statics of the connection truss model (Figure 4) gives:

$$V_c = \frac{M_{pr}}{L-d} = \frac{6{,}793}{84-21} = 108 \text{ kips} \quad (2)$$

$$T = \frac{M_{pr}}{d_b - t_f} = \frac{6{,}793}{20.83 - 0.535} = 335 \text{ kips} \quad (3)$$

$$T + V_c = 335 + 108 = 443 \text{ kips} \quad (4)$$

$$\frac{V_c}{2} = 54 \text{ kips} \quad (5)$$

Thus, the design horizontal and vertical connection reaction forces for each flange of the beam are 443 and 54 kips, respectively.

Assuming the horizontal connection reaction force is equally distributed between the horizontal (cover) plate and the set of four vertical rib plates (two outside the flange and two inside against the beam web), the required area of the horizontal flange plate A_h was obtained as:

$$A_h = \frac{T + V_c}{2\phi F_y} = \frac{443}{2 \times 0.9 \times 50} = 4.92 \text{ in.}^2 \quad (6)$$

where

F_y = yield stress for A572 Gr. 50 plate, taken as 50 ksi

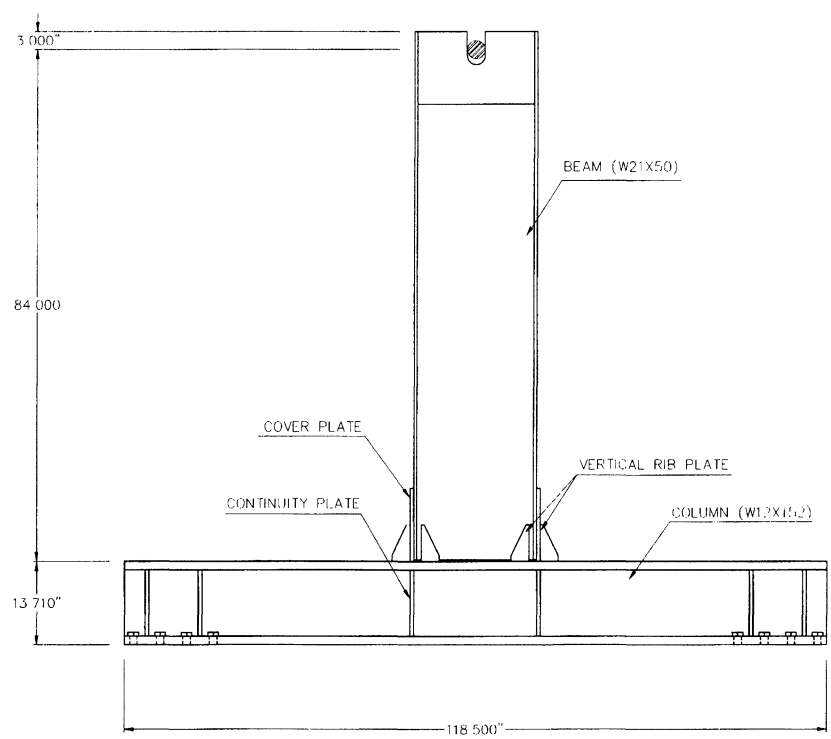

Fig. 6. Final specimen design.

ϕ = resistance factor, taken as 0.9 according to the AISC LRFD Specification

Therefore, 9×12×⅝-in. A572 Gr. 50 cover plates (A_h = 5.625 in^2) were used.

The required area of the four A572 Gr. 50 vertical rib plates, A_v, was calculated for combined normal stress, f_t, due to the horizontal connection reaction force and the shear stress, f_v, due to the vertical connection reaction force.

$$f_t = \frac{0.5(T + V_c)}{A_v} = \frac{0.5 \times 443}{A_v} = \frac{221.5}{A_v} \tag{7}$$

$$f_v = \frac{0.5V_c}{A_v} = \frac{54}{Av} \tag{8}$$

Applying Von Mises' yield criterion with a resistance factor ϕ = 0.9 against yielding, a form of the equation suggested in[17]

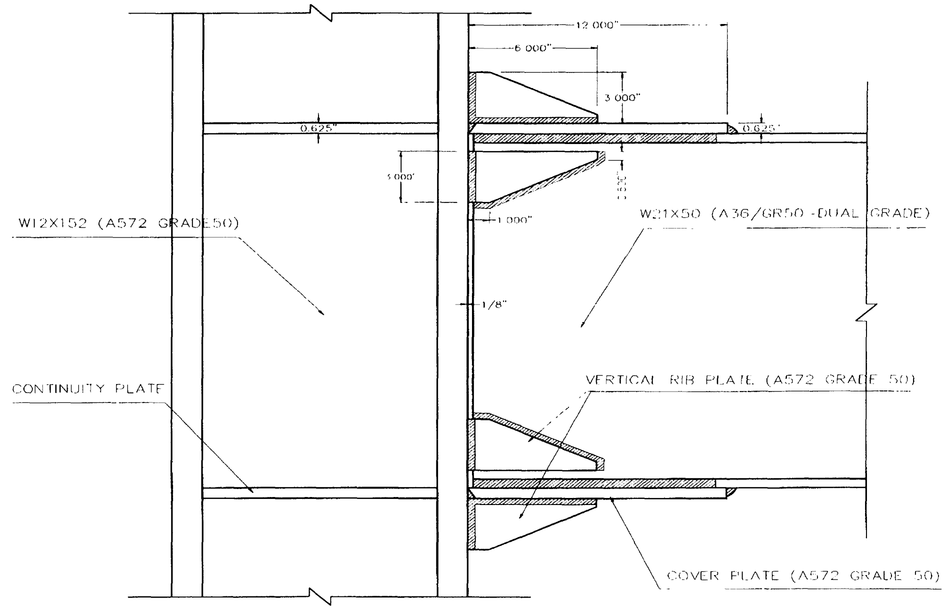

Fig. 7. Elevation view of the specimen connection detail.

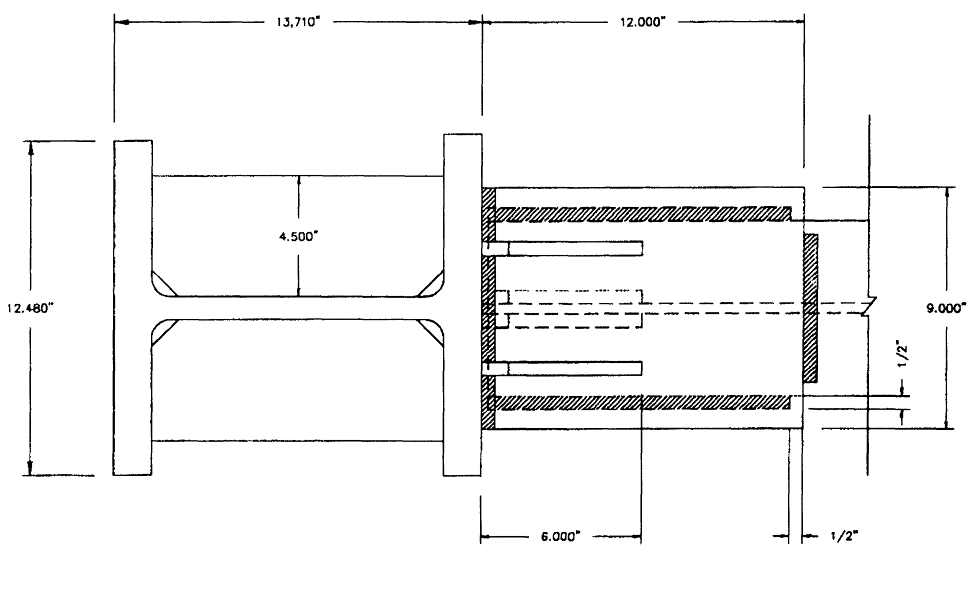

Fig. 8. Plan view of the specimen connection detail.

was used to calculate the required area of the vertical rib plates:

$$f_t^2 + 3f_v^2 = (\phi F_y)^2 \tag{9}$$

$$\left(\frac{221.5}{A_v}\right)^2 + 3\left(\frac{54}{A_v}\right)^2 = (0.9 \times 50)^2 \tag{10}$$

The required area $A_v = 5.34\text{in.}^2$, or 1.32in.^2 for each one of the four vertical rib plates. Therefore, four 3×6×½-in. A572 Gr. 50 triangular rib plates ($A_{v1} = 1.5$ in.^{2}) were used.

All connection plates were fillet welded to the beam. The cover plates were connected to the column using groove welds. The rib plates were welded to the column using fillet welds. The properties of the specimen materials, as measured from coupon tests, are shown in Table 1. All welds were designed using the AISC LRFD Specification assuming the properties of E70 weld material. The weld details are shown in Figures 7 and 8. Welding was performed by a laboratory technician who was not a certified welder, using the Lincoln Electric Idealarc Pulse Power 500 machine with L56.045 wire and a metal-arc inert gas-shielded (MIG) welding process.

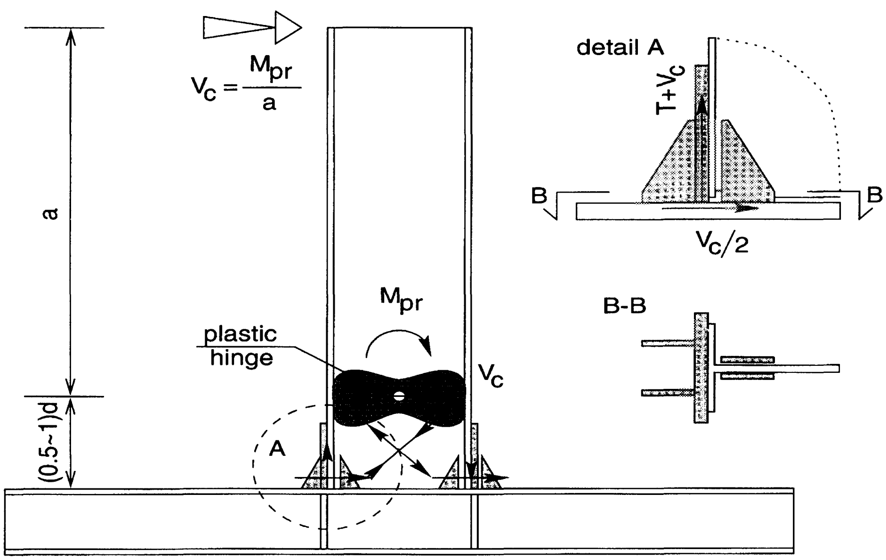

Fig. 9. Connection reaction forces.

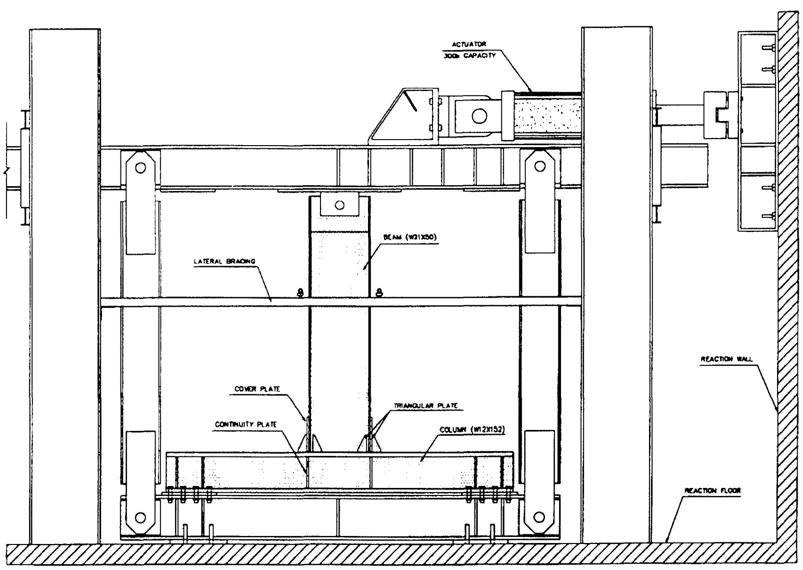

Fig. 10. Test setup.

Table 1. Strengths of the Specimen Materials					
[ksi]	Beam Web	Column Web	Column Flange	Cover Plate	Vertical Rib
F_y	43	59	42	56	63
F_u	62	73	64.5	77	78

Table 2. Typical Mechanical Properties of the Welds				
Yield Strength [ksi]	Tensile Strength [ksi]	Elongation [% in 2-in.]	Charpy V-notch [ft-lbs]	
			0°F	−20°F
60 (min)	72 (min)	22 (min)	not specified	20 (min)

The typical mechanical properties of the welds using this wire following ER705-6 per AWS A5.18 are specified by the manufacturer and shown in Table 2.

TEST RESULTS

The specimen was rotated 90 degrees with respect to its position in a building and placed into the loading frame (Figure 10). The free end of the beam was attached to the actuated part of the frame.

The loading frame braces allowed for in-plane motion while preventing out-of-plane deformation of the beam.

The specimen was tested by applying a displacement pattern (Figure 11) to the top of the beam. The displacement pattern has two parts. The first, ascending, part of the pattern was constructed following the ATC-24[25] recommendations and the SAC Joint Venture Steel Project guidelines.[3] The second, descending, part of the pattern was designed to test the behavior of the severely damaged specimen. The defining parameter of the displacement pattern, the specimen yield displacement, was determined using a finite element model. The analysis showed that significant yielding across the entire depth of the beam flange occurred at the beam tip displacement of 0.6 inch. This value was used to calculate the magnitude of displacements in the test pattern.

The first sign of local strain concentration at the bottom surface of the beam flanges, approximately 9 inches away from the column flange, was observed during the 0.45 inch ($0.75\delta_y$) load cycle. Beginning of the inelastic behavior of the specimen, indicated by a slight widening of the hysteresis loops in the force-displacement graph (Figure 12), occurred during the 0.6 inch ($1\delta_y$) load cycle. The peak force achieved in this cycle was 58.4 kips. The corresponding story drift was 0.71 percent.

Spalling of the whitewash and mill scale on the bottom of the beam flange approximately 3 inches away from the end of the cover plate was the first visual sign of yielding. It, too, occurred during the 0.6 inch ($1\delta_y$) load cycle. Development of the beam plastic hinge, centered approximately 16 inches away from the column flange, continued during the subsequent load cycles. The process of plastification was characterized by propagation of the yield pattern upwards along the beam flanges and by yielding of the beam web (Figure 13). The energy dissipated though plastification is reflected in wider hysteresis loops and smaller specimen stiffness (Figure 12).

The ultimate resisting force of the specimen was 89.9 kips. It was attained at the first peak displacement of the 1.8 inch

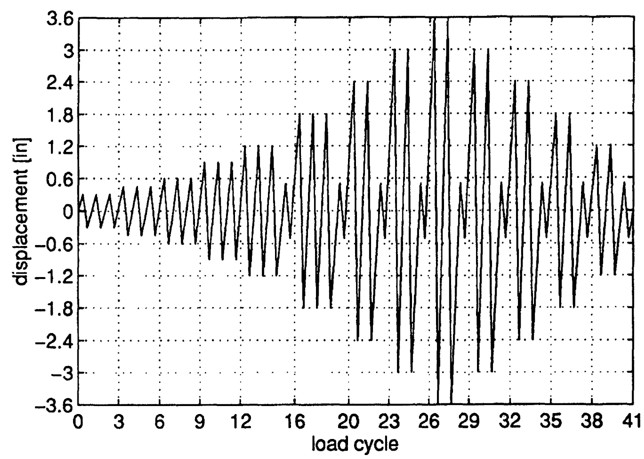

Fig. 11. Applied displacement pattern.

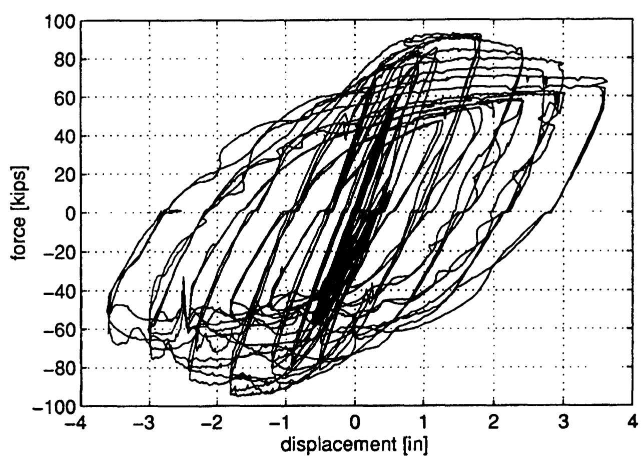

Fig. 12. Force-displacement response of the specimen.

($3\delta_y$) load cycle. The horizontal drift of the specimen at the ultimate resistance point was 2.14 percent. The resistance of the specimen was limited by local buckling of the beam. The instability apparently started in the portion of the beam web in compression, followed by buckling of the compression beam flange. The ultimate resistance of the specimen was estimated at approximately 92 kips, using a non-linear small displacement finite element model.

At this point in the test, the areas of the specimen away from the plastic hinge zone were carefully inspected for signs of yielding or damage. Several yield lines were observed on the cover plates in the area between the triangular plates, on the bottom of the beam flange in the area between the end of the cover plate and the beginning of the triangular plates and near the top corner of the outside triangular plates. There were no signs of yielding in the column. Visual inspection showed no damage in any of the welds.

Local buckling of the flanges in the plastic hinge region of the beam dominated subsequent response of the specimen. The resistance of the specimen dropped by approximately 8 percent of the ultimate value in each new displacement cycle, tracing a negative stiffness region of the force-displacement response envelope. However, the repeated hysteretic loops at each new displacement level were stable and full. Increasing deformation demands were accommodated by severe local buckling of the beam and by spreading of the plastic deformation zone away from the connection. The overall deformed shape of the beam is shown in Figure 14.

The applied displacement increase continued up to the 3.6 inch (4.31 percent drift) level. The plastic rotation of the specimen reached 0.044 radian, a level that exceeded the rotation recommendation for beam-column connections[2] by approximately 50 percent. A total of 40 displacement cycles wit normalized cumulative ductility of $218\delta_y$ was applied to the specimen. The specimen resistance at this point was 66.7 kips, 74 percent of the ultimate resistance value.

The descending portion of the test pattern was applied at this time. The response of the specimen was stable and repeatable at each displacement level. The response of the buckled specimen was stable, albeit with somewhat smaller stiffness and strength than the specimen at the beginning of the test. Spalling of whitewash at the diagonal welds of the inside triangular plates was the only change observed during this part of the test (Figure 15).

SUMMARY AND CONCLUSION

Beam-to-column moment connections in steel frames have been traditionally designed by using the classical Euler-Bernoulli beam theory which assumes that the flanges primarily transfer moment while the web connection primarily resists the shear force. The results of finite element analysis briefly presented in this paper have shown that stress pattern in the vicinity of moment connections changes drastically from that suggested the beam theory. This is in agreement with the boundary effects as postulated in the Saint Venant's Principle. The magnitude and direction of principal stresses in the connection region are better approximated by using truss analogy. Accordingly, the shear force is also transferred to the connection near the flanges through diagonal strut action, thus, overloading those regions.

Using the finite element analysis results and the truss model, a practical and more rational analysis and design procedure is proposed. The new connection design uses a combination of flange cover plates and vertical rib plates to carry the normal and shear stresses created by the truss action. The design procedure was applied and successfully validated through cyclic load testing of a nearly full size specimen. The connection withstood more than 40 cycles of displacement up to a maximum story drift of over 4 percent and a plastic rotations in excess of 0.04 radian. As intended by design, the plastic hinge formed in the beam away from the connection with no significant yielding in the connection region. The test was stopped after severe local buckling in the beam. Even after a rather demanding deformation history applied to the specimen no cracks could be seen anywhere.

The successful application of truss analogy to design and analysis of steel beam-to-column moment connections as presented in this paper is very encouraging. It shows that choice of a realistic load transfer model provides a clear understanding of the function of each element of the connection and leads to a rational design procedure. The principles presented in the paper are general with possible application to other connection situations, such as column bases, eccentrically loaded brackets, bases of shear walls, and gusset plates, under static as well as dynamic loads. It should be noted, however, that the conclusions presented in this paper are based on a very limited analytical and experimental study,

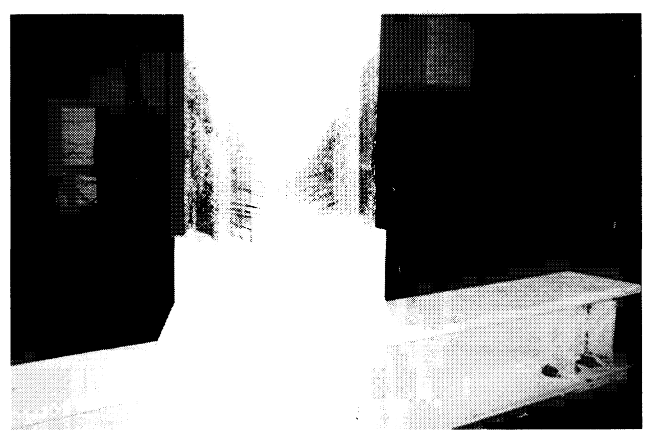

Fig. 13. Propagation of the yield pattern and absence of damage in the connection region.

consisting of only one analytical prototype and one test specimen. A much broader study is needed before the truss analogy concept and the design procedure can be generally accepted in practice.

REFERENCES

1. Goel, S. C., Stojadinovic, B., and Lee, H.-K., "A New Look at Steel Moment Connections," *Technical Report UMCEE 96-19*, Department of Civil and Environmental Engineering, the University of Michigan, August, 1996.
2. Federal Emergency Management Agency, *Interim Guidelines: Evaluation, Repair, Modification and Design of Welded Steel Moment Frame Structures*, 1995, Report FEMA-267.
3. SAC Joint Venture, "Experimental Investigation of Beam-Column Subassemblages: Part 1 and Part 2, 1996," *Report SAC-96-01, Part 1 and Part 2.*
4. Engelhardt, M. D. and Sabol, T. A., "Testing of Welded Steel Moment Connections in Response to the Northridge Earthquake," *Progress report*, AISC Advisory Subcommittee on Special Moment Resisting Frame Research, October, 1994.
5. Bertero, V. V., Anderson, J. C., and Krawinkler, H., "Performance of Steel Building Structures During the Northridge Earthquake," *Technical Report UCB/EERC 94/09*, Earthquake Engineering Research Center, University of California, Berkeley, 1994.
6. SAC Joint Venture. *Surveys and Assessment of Damage to buildings Affected by the Northridge Earthquake of January 17, 1994*, Report SAC-95-06, 1995.
7. Holmes, W. T. and Sommers, P., "Northridge Earthquake of January 17, 1994: Reconnaissance Report," *Earthquake Spectra*, Vol. 11, 2C, 1996.
8. Shedd, T. C., *Structural Design In Steel.* John Wiley & Sons, Inc., 1934.
9. Abel, J. F. and Popov, E. P., "Static and Dynamic Finite Element Analysis of Sandwich Structures," In *Proceedings of Second Conference on Matrix Methods in Structural Analysis*, pp. 232, Air Force Flight Dynamics Laboratory and Air Force Institute of Technology, December, 1969.
10. Popov, E. P. and Pinkney, R. B., "Cyclic Yield Reversal in Steel Building Connections," *Journal of The Structural Division*, ASCE, 95(ST3):327-353, March 1969.
11. Popov, E. P. and Stephen, R. M., "Cyclic Loading of Full Size Steel Connections," *Technical Report UCB/EERC-70/03*, Earthquake Engineering Research Center, University of California, Berkeley, 1970.
12. Timoshenko, S. and Goodier, J. N., *Theory of Elasticity*, McGraw-Hill Book Company, 2nd Ed., 1951.
13. Yang, T.-S. and Popov, E. P., "Behavior of Pre-Northridge Moment Resisting Steel Connections," *Technical Report UCB/EERC-95/08*, Earthquake Engineering Research Center, University of California, Berkeley, 1995.

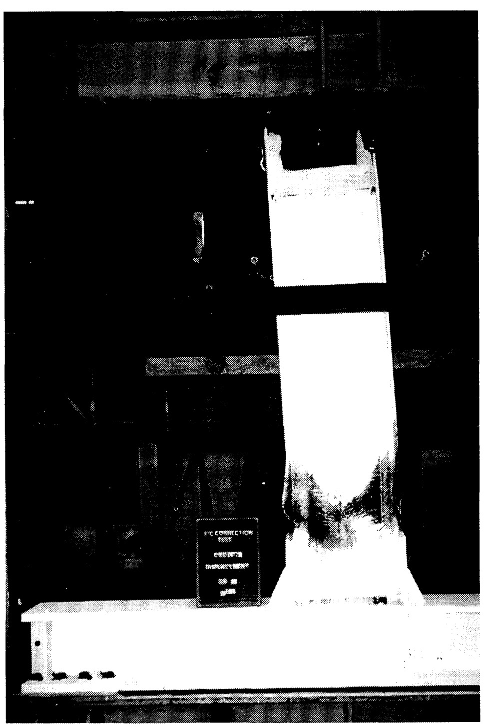

Fig. 14. Overall deformation of the specimen.

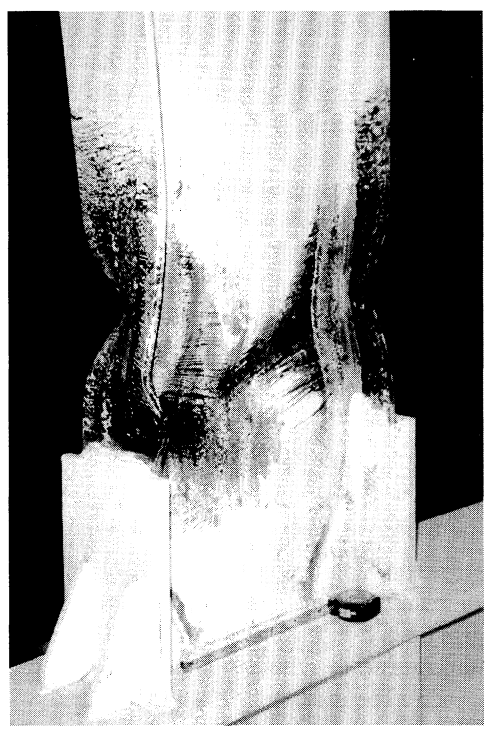

Fig. 15. Specimen at the end of the test.

14. Allen, J., Partridge, J. E., and Richard, R. M., "Stress Distribution in Welded/Bolted Beam to Column Moment Connections," *Technical report*, The Allen Company, 1995.
15. Schlaich, J., Schafer, K., and Jannewein, M., "Toward a Consistent Design of Structural Concrete," *PCI Journal*, 32(3):77-150, May/June, 1987.
16. American Concrete Institute. *Building Code Requirements for Structural Concrete (ACI318-95) and Commentary (ACI 318-95R)*, 1995.
17. Astaneh-Asl, A., "Simple Methods for Design of Gusset Plates," In Iffland, J. S. B., color, ASCE *Steel Structures, Proceedings of ASCE Structures Congress*, pp. 345–354, May 1989.
18. Bursi, O. S., "Elastic-Plastic Modeling of Structural Fasteners for Steel Bracing Connections," *Journal of Constructional Steel Research*, 30:13-38, 1994.
19. Bursi, O. S., Gerstle, K. H., Sigfusdottir, A., and Zitur, J. L., "Behavior and Analysis of Bracing Connections for Steel Frames," *Journal of Constructional Steel Research*, 30:39–60, 1994.
20. Miller, D. K., "Lessons Learned from the Northridge Earthquake," In Chen, W. F. and White, D. W., editors, *Innovations in Stability Concepts and Methods for Seismic Design in Structural Steel*, June 1996. U.S./Japan Seminar.
21. Iwankiw, N., "Ultimate Strength Considerations for Seismic Design of the Reduced Beam Section (Internal Plastic Hinge)," AISC *Engineering Journal*, 1st Qtr., 1997, pp. 3–16.
22. American Institute for Steel Construction, *Load and~ Resistance Factor Design*, 2nd Ed., 1994.
23. Goel, S. C., "Combined Shear and Tension Stresses," AISC *Engineering Journal*, 4th Qtr., 1986, pp. 124–125.
24. Lincoln Electric, *Lincolnweld L-50, L-50B, L-54, L-54B, L-56, L-56 Gas Metal Arc Welding Electrodes AWS ER70S-3, ER70S-4, ER70S-6*, June, 1992.
25. Krawinkler, H., "Guidelines for Cyclic Seismic Testing of Components of Steel Structures," *Technical Report ATC-24*, Applied Technology Council, 1992.